# Prediction of Separated Asymmetric Trailing-Edge Flows at Transonic Mach Numbers

C. C. Horstman*
*NASA Ames Research Center, Moffett Field, California*

**Numerical simulations of the time-dependent, Reynolds-averaged, Navier-Stokes equations, employing various eddy viscosity turbulence models are presented and compared with measurements from an investigation of a transonic trailing-edge flow at a high Reynolds number. Comparisons are made for mean surface quantities as well as mean and fluctuating flowfield quantities. Solutions employing two-equation turbulence models correctly predict all the major features of the flowfield. Viscous/inviscid interaction effects were found to be extremely important for predicting this flowfield and equally important to the turbulence modeling employed.**

## Nomenclature

$C_{f_e}$ = skin-friction coefficient based on boundary-layer edge conditions
$k$ = turbulent kinetic energy
$p$ = pressure
$u$ = velocity in $x$ direction
$u_0$ = sonic (reference) velocity
$v$ = velocity in $y$ direction
$w$ = velocity normal to $u$ and $v$
$x$ = streamwise coordinate parallel to model centerline measured from model trailing edge
$y$ = vertical coordinate normal to model centerline measured from model surface and in the wake from the extension of the model trailing edge
$\delta^*$ = boundary-layer displacement thickness
$\epsilon$ = turbulence energy dissipation
$\theta$ = boundary-layer momentum thickness
$\mu$ = molecular viscosity
$\rho$ = density
$\tau$ = shear stress
$\omega$ = turbulent dissipation rate

*Subscripts*

$T$ = total
$w$ = wall conditions

*Superscripts*

$( )'$ = fluctuating quantity
$\langle ( ) \rangle$ = rms value

## Introduction

THE capability to predict the flow about the trailing edge and in the near wake of an airfoil plays a critical role in the airfoil design process. For modern supercritical airfoils the trailing-edge region is dominated by viscous/inviscid interaction effects, large streamwise adverse pressure gradients, large pressure gradients normal to the airfoil surface and, for many cases, separated flow.[1-4] In the near wake the flowfield is complicated by streamline curvature and by the interaction of two significantly different shear layers. To adequately predict an airfoil's performance, a successful calculation method must model all of these effects.

In the past several years, considerable advances have been made in the prediction of attached transonic trailing-edge flows. Integral boundary-layer methods coupled with an inviscid flowfield solution have been successfully applied to both symmetric and asymmetric trailing-edge flows provided there is no boundary-layer separation.[1,3,5] These methods are not satisfactory for flows with strong adverse pressure gradients leading to significant separated regions.[3,6] Differential methods employing either a boundary-layer code coupled with an inviscid solution or the mass-averaged Navier-Stokes equations throughout the flowfield have also been successful provided separation was not present.[5,7] The ability to calculate separated trailing-edge flows remains to be tested.

The importance of predicting the near-wake region is not critical for predicting an airfoil's performance when a weak interaction is present at the trailing edge. This has been shown by the success of the integral methods which use only an approximate treatment of the wake. The near wake becomes very important when a strong interaction with separation is present because the merging process determines the wake closure that may control the extent of the separated flow on the airfoil and thus the trailing-edge pressure distribution. At present, it appears as if integral or differential boundary-layer methods cannot handle these strong interaction flows.

For flows with no trailing-edge separation and moderate pressure gradients the viscous/inviscid effects are dominant and turbulence modeling may play a secondary role.[5,7] However, for flowfields where large separated regions are present, turbulence modeling becomes extremely important.[5] Further progress in calculating separated flows relies heavily on extracting information relevant to turbulence modeling from well-planned experiments involving turbulence measurements. A recent experimental investigation performed at NASA Ames Research Center[8] has provided an excellent test case for asymmetric trailing-edge flows with a small-scale separation. The measurements included both mean and fluctuating flowfield quantities in sufficient detail to allow a proper assessment of the turbulence modeling employed in the calculation method.

This paper presents a detailed comparison between numerical calculations and the experimental results for the asymmetric trailing-edge flow case as described above. The computed results are solutions of the time-dependent, Reynolds-averaged, Navier-Stokes equations which use either algebraic or two-equation eddy-viscosity turbulence models. By employing the Navier-Stokes equations throughout the flowfield, the near-wake merging process is properly calculated and the effects of normal pressure gradient, viscous/inviscid interactions, and ellipticity of the flow are

Presented as Paper 82-1021 at the AIAA/ASME Third Joint Thermophysics, Fluids, Plasma and Heat Transfer Conference, St. Louis, Mo., June 7-11, 1982; submitted June 17, 1982; revision submitted Dec. 17, 1982. 

*Assistant Chief, Experimental Fluid Dynamics Branch. Associate Fellow AIAA.

automatically included. The emphasis of this paper is to assess the effect of turbulence modeling in solving this complex flow. Also, the effects of streamline curvature, which is thought to be an important feature for separated trailing-edge flows, are evaluated. Based on these comparisons, the deficiencies in various turbulence models are discussed and recommendations are then made for obtaining the correct solution of an asymmetric trailing-edge flow.

## Experiment Description

The experiment was performed in the Ames High Reynolds Number Facility (38.1×25.4 cm) at a nominal freestream Mach number of 0.7 and a freestream unit Reynolds number of $4.0\times10^7$/m. A sketch of the flow geometry is shown in Fig. 1. The cross section of the trailing-edge region is the upper rear quadrant of an 18% thick circular arc airfoil; the arc has a radius of 40.4 cm and the trailing-edge included angle of the flap is 20.4 deg. Thick turbulent boundary layers developed on both sides of the model, which merged at the trailing edge, forming an asymmetric wake. A small separation zone was obtained over the final 2 cm of the upper surface. Two-dimensionality was verified with surface oil flow patterns, spanwise flowfield measurements, and momentum integral balances using the measured data.

The measurements included surface pressure, skin friction, mean flowfield pressure and velocity distributions, and fluctuating velocity and shear stress data throughout the flowfield. The skin-friction data were obtained from law-of-the-wall correlations. The mean velocity data were obtained from pitot-static pressure probes. A two-color laser Doppler velocimeter was used to measure both the mean and fluctuating flowfield. Flowfield measurements were obtained over the trailing edge of the flap and in the near wake extending from $x=\mp7.5$ to 12.5 cm. Further details of the experimental techniques, accuracy of the measurements, and results are contained in Ref. 8.

## Solutions to the Navier-Stokes Equations

The partial differential equations used to describe the mean flowfield are the time-dependent, Reynolds-averaged, Navier-Stokes equations for two-dimensional flow of a compressible fluid. Restrictions on the equations include the perfect gas assumption, constant specific heats, the Sutherland viscosity law, and zero bulk viscosity. Several eddy-viscosity models were chosen for evaluation in the turbulence closure: the algebraic model developed for near-wake flows by Cebeci,[9] the two-equation $k$-$\epsilon$ model,[10] and the two-equation $k$-$\omega^2$ model.[11] Modifications to the $k$-$\epsilon$ model proposed by Chien[12] to model the low Reynolds number near-wall terms were also employed. Two methods were used to correct the turbulence model equations for streamline curvature: one by Launder et al.[13] that makes a modification to the $\epsilon$ equation and the other proposed by Cousteix[5] that applies a correction to the Reynolds shear stress. The $k$-$\omega^2$ model differs from most other eddy-viscosity models in that the constitutive relation between the Reynolds stress tensor and the mean flow properties has been modified to represent anisotropic normal Reynolds stress phenomena. When the two-equation turbulence models are used, the Navier-Stokes equations are augmented by two additional partial differential equations. The complete equations, including the equations and constants for each turbulence model, are described in Refs. 9, 11, 12, and 14.

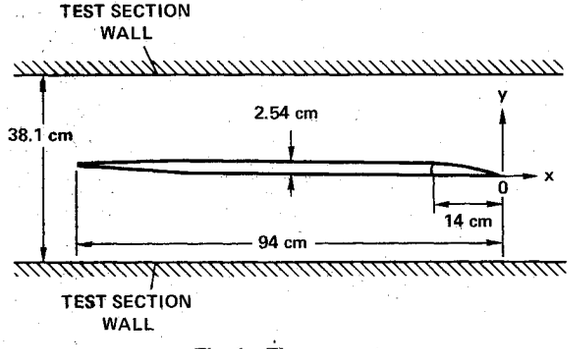


Fig. 1 Flow geometry.

The numerical procedure used here is the basic explicit second-order, predictor-corrector, finite-difference, time-splitting method of MacCormack, modified by an efficient implicit algorithm.[15]

The computational domain extended in the streamwise direction from $x=-50$ to 65 cm and in the vertical direction to include both test section walls. A mesh was developed that allowed a variable point spacing in each coordinate direction. One set of grid lines was placed normal to the freestream direction and the other parallel to the model surface and wake centerline. The total mesh size was 79 points in the streamwise direction and 82 points normal to the model surface (41 points on each side). In the streamwise direction mesh spacing varied from 0.08 cm near the trailing edge to 12.5 cm near the downstream boundary. In the direction normal to the surface, an exponentially stretched spacing was used near the wall followed by a uniform spacing. The distance of the first $y$ mesh point from the model wall was selected small enough so that the solutions are independent of spacing (typically within $y^+_{\min}\equiv y\sqrt{\tau_w\rho_w/\mu_w}<1.0$).

The upstream boundary conditions were prescribed by a combination of uniform freestream conditions and the result of a boundary-layer computation[11] along the model surface. The downstream boundary was positioned far enough aft so that all of the gradients in the streamwise direction could be set to zero. This boundary condition was verified by the lack of any substantial change in the numerical results when the location of the downstream boundary was changed. At the model surface, no-slip boundary conditions are applied along with a constant wall temperature. For the two-equation closure models the turbulent kinetic energy and dissipation rate $\epsilon$ was set equal to zero at the wall. In addition, the $k$-$\omega^2$ model used an analytic expression for $\omega^2$ at the wall.[11,14] At the upper and lower boundaries (the parallel wind tunnel walls), inviscid solid-wall boundary conditions were used.

## Results and Discussion

Several solutions have been obtained for the trailing-edge flowfield under investigation. Only minor differences were discovered between the various two-equation turbulence model solutions independent of the near-wall treatment of the low Reynolds number terms and the inclusion of corrections for streamline curvature. However, larger differences were found between solutions using the two-equation and the algebraic eddy-viscosity models. The best results when compared to experiment were obtained by the original $k$-$\epsilon$ model[10] with the streamline curvature correction to the Reynolds stress as suggested by Cousteix.[5] In the following discussion, this solution will be compared in detail with the experimental results. Then for a few selected survey stations, where the greatest differences between solutions occur, the computed results for the various turbulence models will be compared with the experimental data. Finally, computed results for the displacement thickness using boundary-layer codes will be compared with the present Navier-Stokes calculations.

Figure 2 compares the computed and experimental wall pressure distributions on the test model. The agreement is very good. Note that the computed pressure is slightly higher than the measured pressure on the upper surface ahead of the hinge line. When computing this flowfield it was found that the upper surface freestream Mach number had to be lowered to 0.85 from the quoted experimental value of 0.87 to prevent

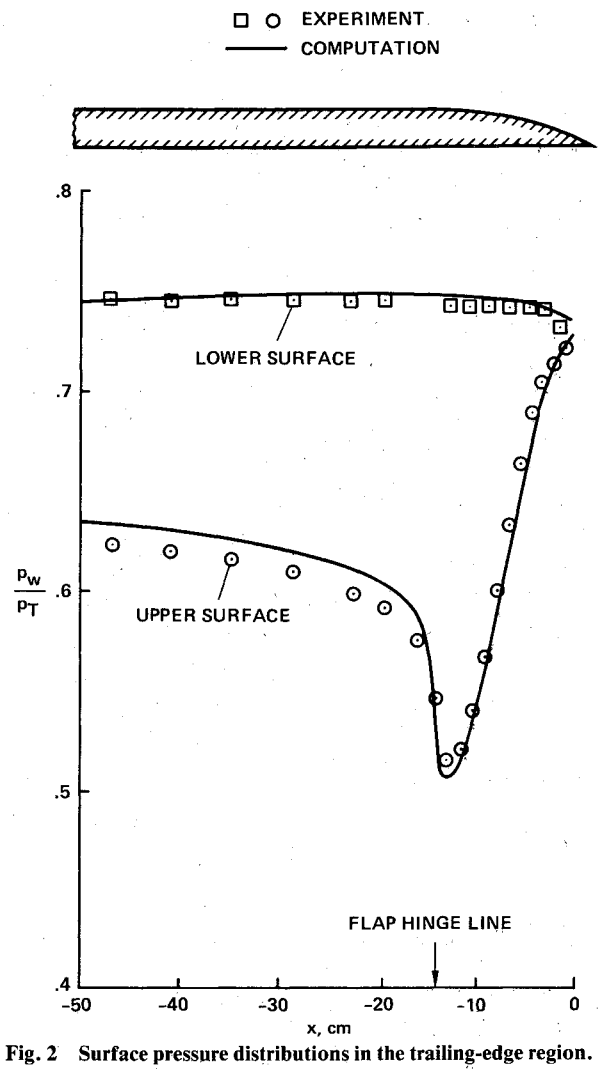


**Fig. 2 Surface pressure distributions in the trailing-edge region.**

a shock wave from forming on the flap. The maximum Mach number in the flowfield is 1.00 for the solution shown, which occurs near the hinge line. The experimenters[8] found that an 0.02 increase of the freestream Mach number also produced a shock wave on the flap. To check whether the boundary-layer growth on the wind tunnel walls influenced the flowfield, a computation was obtained for deflected top and bottom walls accounting for the increasing displacement thickness on the walls. These computed results were essentially identical to those with the nondeflected walls. All the computed surface pressure distributions agreed with each other within 1% independent of the turbulence model used.

Figures 3-5 compare the mean velocity, turbulent shear stress, and turbulent kinetic energy profiles in the trailing-edge and near-wake regions. To obtain $\langle u'^2+v'^2\rangle$ from the computed value of turbulent kinetic energy, it was assumed that $\langle w'^2\rangle = \frac{1}{2}\langle u'^2+v'^2\rangle$. An excellent agreement is observed between the computed and measured mean-velocity profiles (Fig. 3). Also, good qualitative agreement is seen for the turbulent shear-stress (Fig. 4) and kinetic energy (Fig. 5) comparisons. For the wake at $x=5.08$ and 12.07 cm the magnitude of the computed shear-stress and kinetic energy profiles are slightly less than and do not fill out as fast as the measured values. It has been shown[16] that the asymptotic growth rate of the far wake is underpredicted when employing any of the turbulence models used in the present work. Although the present results do not extend into the far wake, the trends in the comparisons are in agreement with the asymptotic growth rate comparisons of Ref. 16.

The displacement thickness on the airfoil is the most critical viscous parameter to correctly predict for the airfoil designer who uses interactive procedures. This displacement thickness is necessary to predict the pressure distribution and thus the lift and drag. Comparisons of the present computations with experimental values of displacement and momentum thickness on the upper model surface are shown in Fig. 6. These comparisons show good agreement. To calculate $\delta^*$ and $\theta$ the pressure variation across the boundary layer was taken into account in the same manner as the experimental procedure.[8] The boundary-layer edge was defined at the first

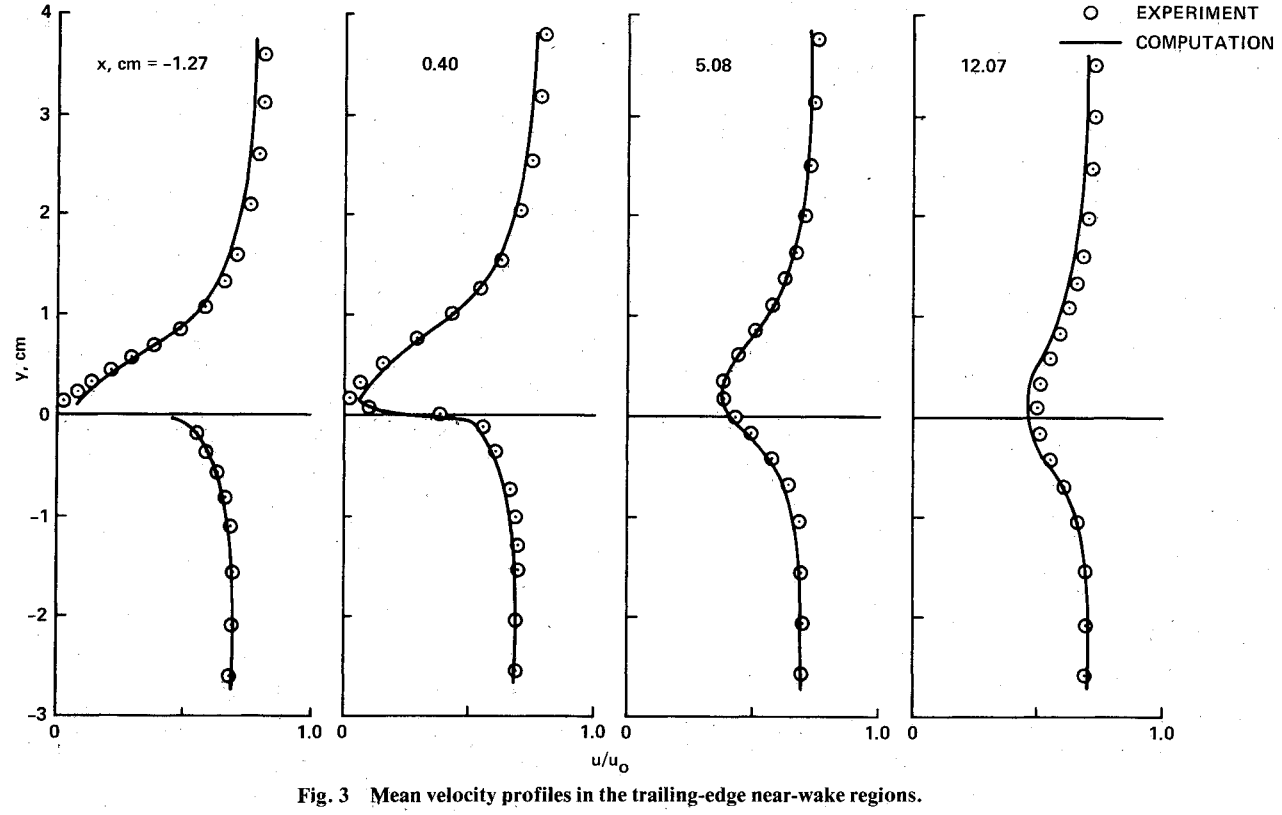


**Fig. 3 Mean velocity profiles in the trailing-edge near-wake regions.**

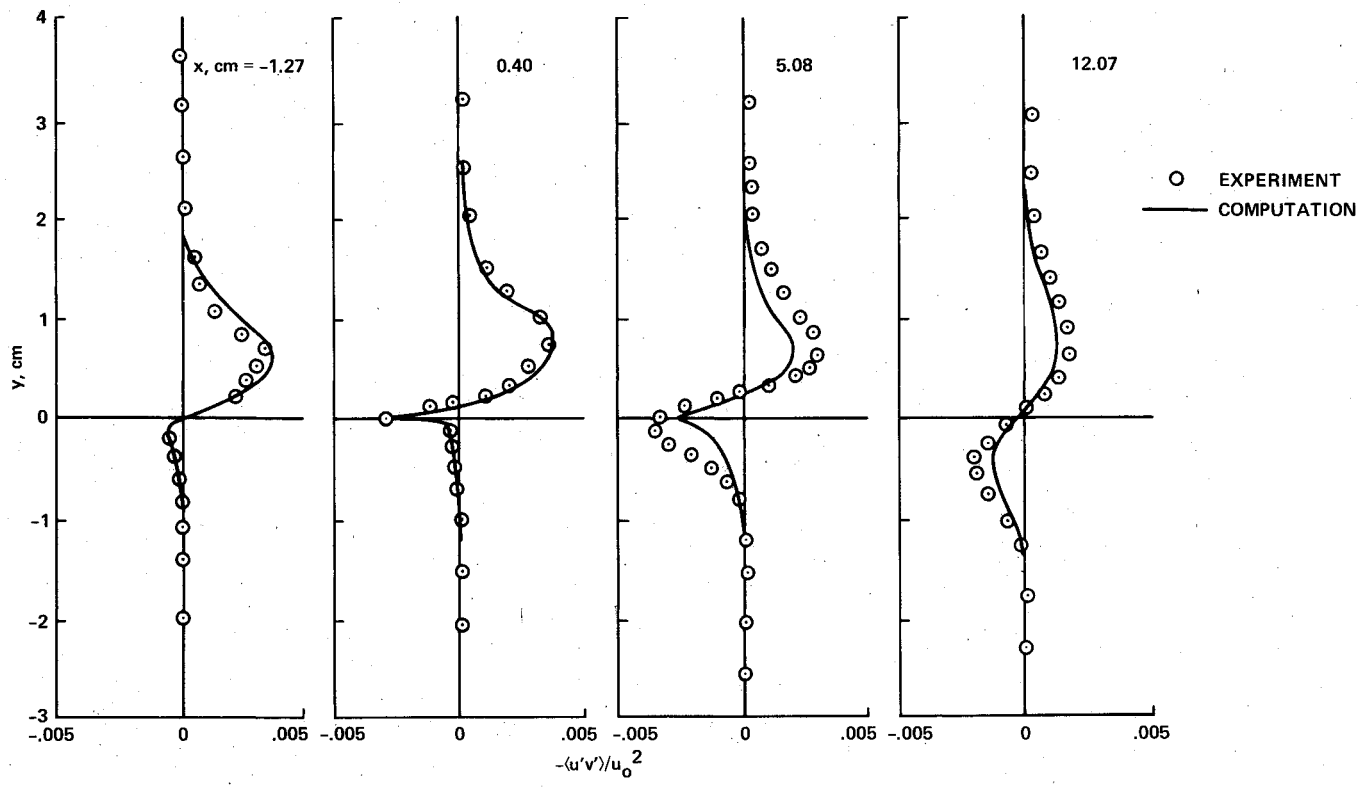


**Fig. 4 Turbulent shear-stress profiles in the trailing-edge and near-wake regions.**

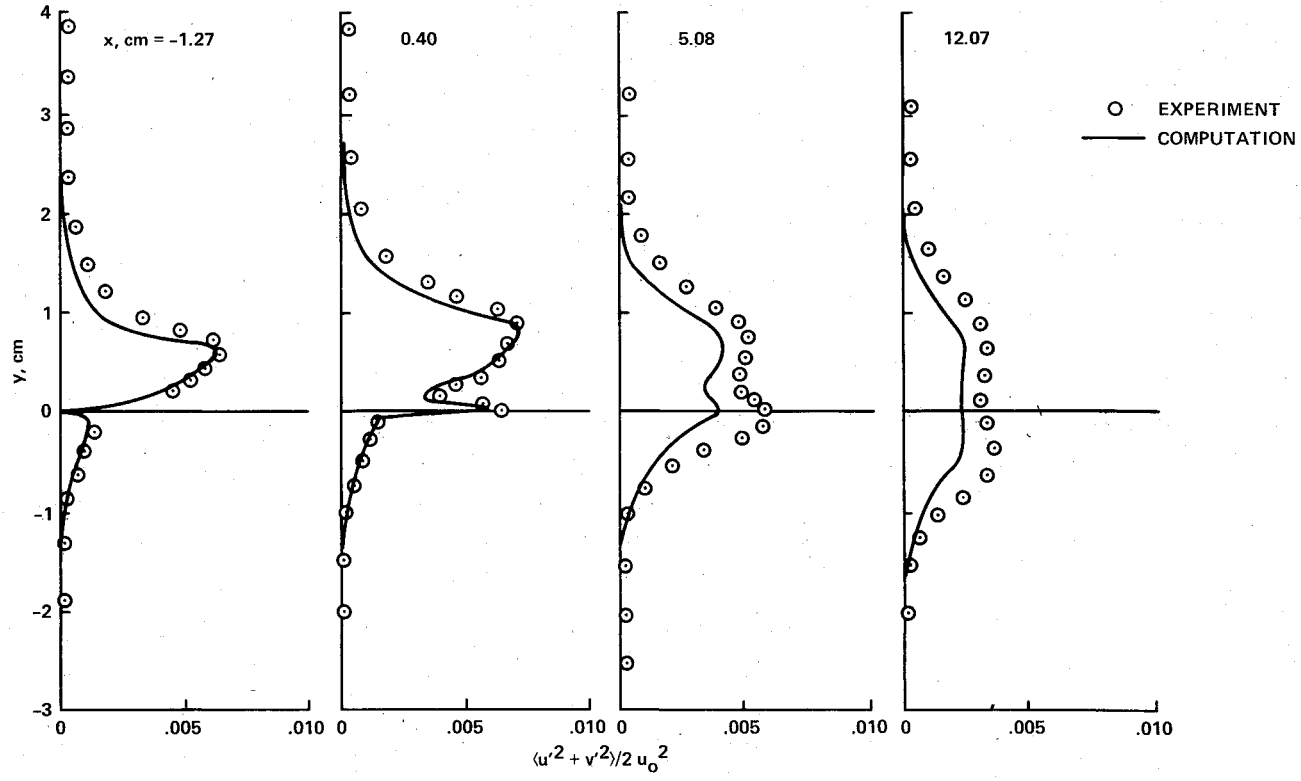


**Fig. 5 Turbulent kinetic energy profiles in the trailing-edge and near-wake regions.**

grid point where the computed total pressure was 99% of the asymptotic value.

The computed skin-friction distribution on the upper surface of the test model is compared with the experimental values in Fig. 7. The scatter bars on the experimental data points represent experimental uncertainty. The computed values are in fair agreement with the data. The measured separated zone extended from $-2$ cm on the flap to 0.4 cm in the wake. The computed separated zones were all significantly smaller. All of the two-equation model solutions had separated zones extending from $-0.25$ to 0.1 cm. The separated zone for the algebraic model solution extended from $-0.9$ to 0.1 cm. The predicted skin-friction distributions from all of the solutions agree within a few percent of the one shown that underpredicts the data at $x = -10$ cm and overpredicts the data at $x = -9$ and $-6$ cm.

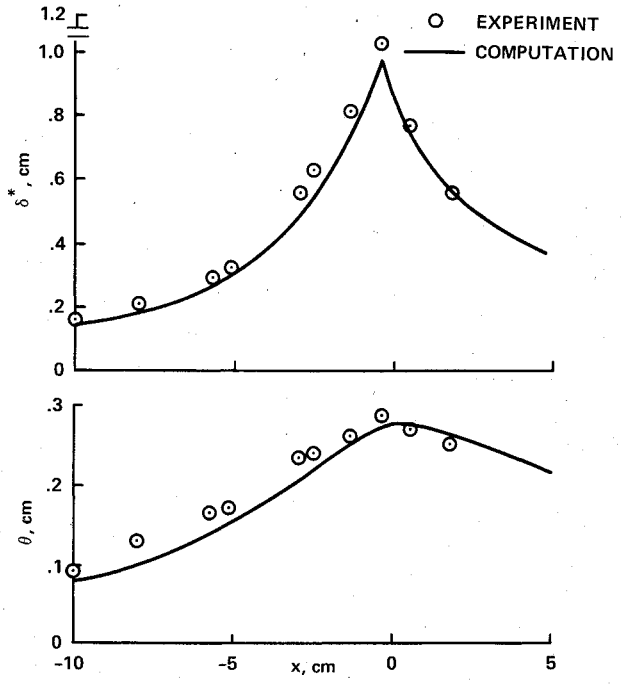


**Fig. 6 Displacement and momentum thickness distributions in the trailing-edge and near-wake regions.**

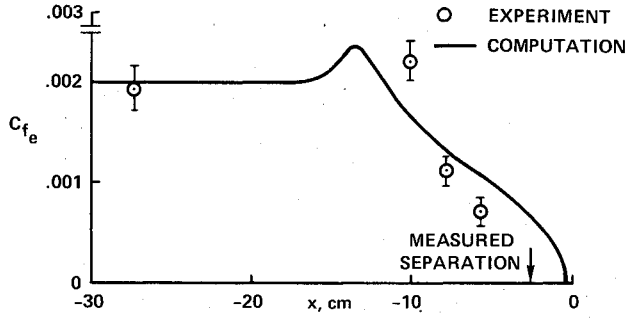


**Fig. 7 Skin-friction distribution in the trailing-edge region.**

Computed results for various turbulence models are compared with the measured mean-velocity profiles in Fig. 8, the measured turbulent shear-stress profiles in Fig. 9, the measured displacement thickness distribution in Fig. 10, and the measured skin-friction distribution in Fig. 11. The largest differences between the various turbulence models occurred in the survey stations shown ($x = -1.27$ and 0.40 cm). For the mean-velocity profiles (Fig. 8) the $k$-$\epsilon$ and $k$-$\omega^2$ results are essentially the same. The inclusion of curvature only provides a slight improvement. However, the profiles for the algebraic model significantly differ in shape and magnitude from the two-equation results.

For the turbulent shear-stress results (Fig. 9), all solutions reasonably approximate the data at $x = -1.27$ cm. At $x = 0.40$ cm the various two-equation models all give good agreement with the data but the algebraic model shows fairly large differences. In the near wake, the algebraic model becomes more complicated because it requires a division of the wake into upper and lower halves about the minimum velocity location and an assumed complex variation of eddy viscosity both normal to and along the wake centerline. In view of the better agreement which was achieved with the two-equation models, the use of an algebraic model to solve this type of flowfield does not seem practical, due to the additional assumptions that are required.

For the predicted displacement thickness distribution (Fig. 10), the various two-equation models all give similar results. The computed distribution using the algebraic model shows larger disagreement with the data, which is a direct result of the mean-velocity-profile comparisons shown earlier. Far downstream ($x > 5$ cm) all of the turbulence models give similar results for both the displacement thickness and mean-velocity profiles.

The predicted skin-friction distributions are shown in Fig. 11 for two turbulence models. Little difference is noted between the two computations. Distributions predicted by the other two-equation models gave results close to the one shown.

Figure 12 compares the distribution of the experimental displacement thickness with the present computations employing the $k$-$\omega^2$ turbulence model and with the computed

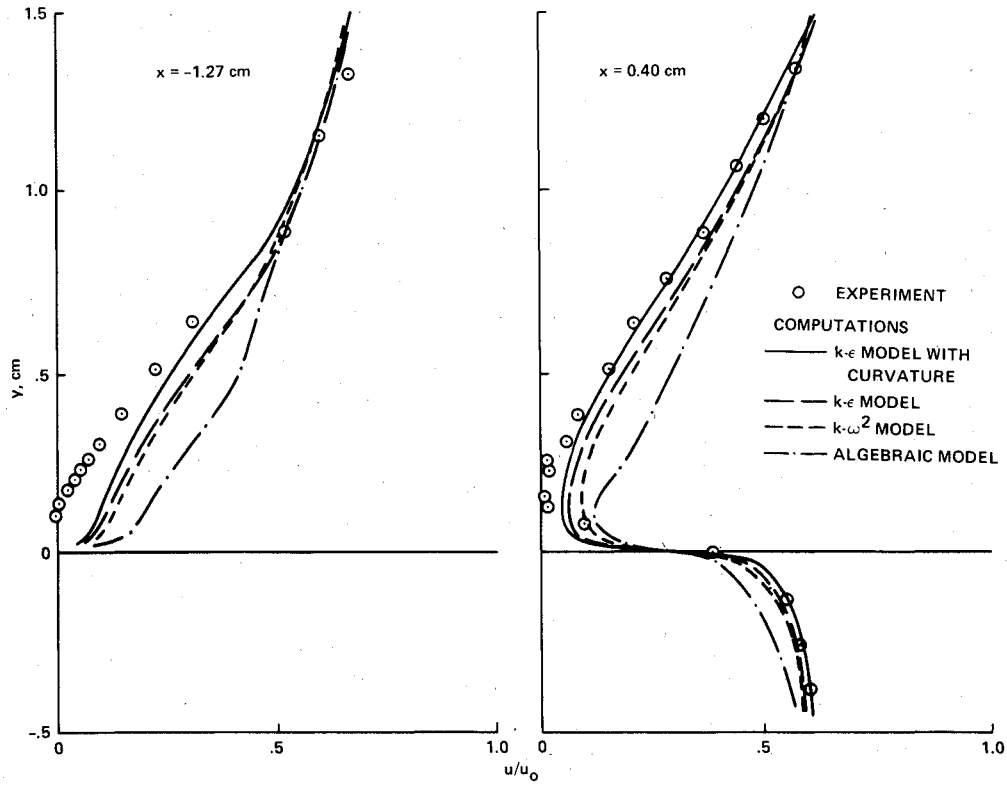


**Fig. 8 Comparison between computations and experimental mean- velocity profiles employing various turbulence models.**

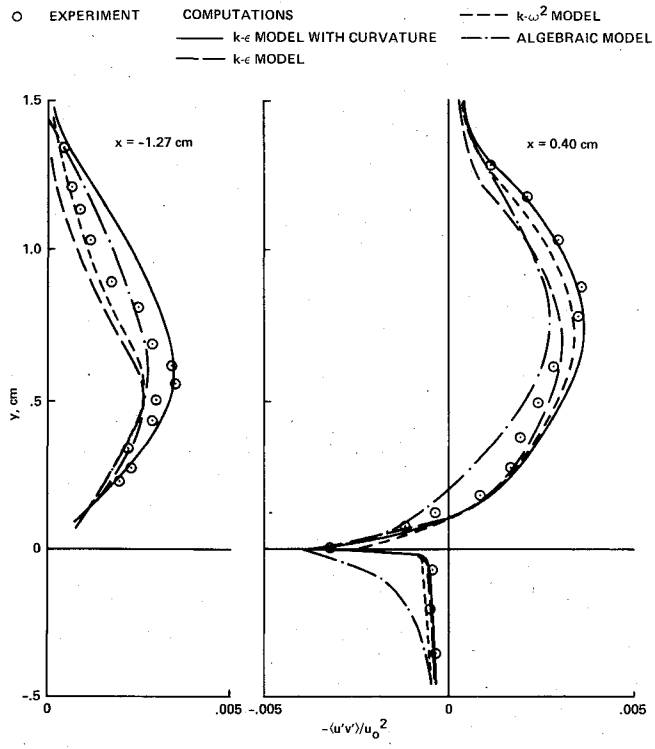


**Fig. 9 Comparison between computations and experimental shear-stress profiles employing various turbulence models.**

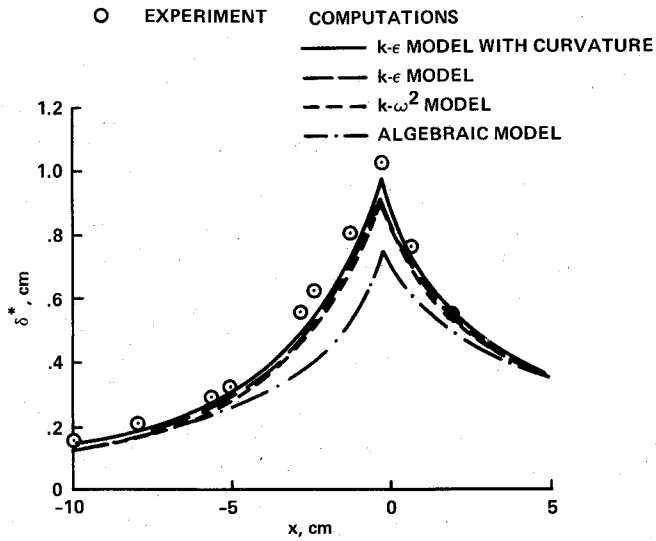


**Fig. 10 Comparison between computations and the experimental displacement thickness distribution employing various turbulence models.**

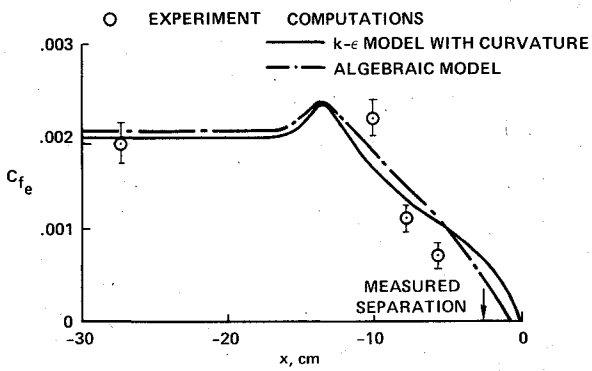


**Fig. 11 Comparison between computations and the experimental skin-friction employing various turbulence models.**

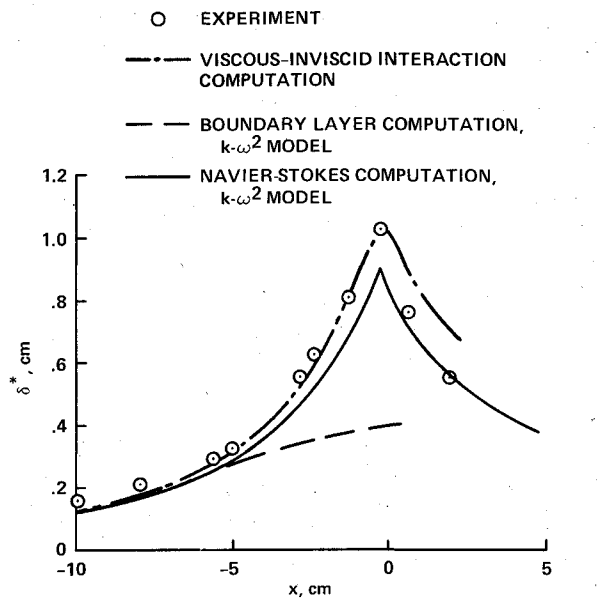


**Fig. 12 Comparison between computations and the experimental displacement thickness distribution employing various computational methods.**

results of a boundary-layer method using the experimentally measured pressure distribution as an input. The $k$-$\omega^2$ boundary-layer method is from Wilcox and Rubesin[11] and it uses the identical model used in the present Navier-Stokes computations. The boundary-layer computation underpredicts the experimental displacement thickness at the trailing edge by 60%, while the present computation is within 10% of the measured values. Based on the use of the same $k$-$\omega^2$ model, it appears as if turbulence modeling is not the cause of these differences. Also shown are the results from a viscous/inviscid interaction method coupling the Euler and momentum and mean-flow kinetic-energy inverse-integral turbulent boundary-layer equations described by Whitfield.[17] The viscous/inviscid interaction results are in good agreement with the data. These results show that the failure of the boundary-layer code[11] to predict the measured data is because of the strong viscous/inviscid interaction process and ellipticity of the flowfield. Evidently for a strong interaction flow such as the present trailing-edge flowfield, the boundary-layer solution is extremely sensitive to the streamwise flow gradients; hence, both the viscous and inviscid portions of the flowfield must be solved interactively. The turbulence model used in the integral boundary-layer equations[17] is based on correlations of experimental data and would be expected to correctly model flowfields where these correlations are valid. The present case with a small separated zone is such a flowfield. However, the extension of this method to flowfields with large separated zones will require additional data correlations not yet available.[17]

Another difference between boundary-layer and Navier-Stokes computations is the inclusion of the streamwise turbulent normal stress gradients in the Navier-Stokes computations. The experimental results[8] have suggested that these terms are important and should be included in the computation. To verify this, the present Navier-Stokes solution was resolved with all the normal stress terms set equal to zero. Since no significant differences from the present results were obtained, we conclude that these terms do not account for the differences between the boundary-layer and Navier-Stokes computations.

## Conclusions

The separated transonic flowfield about an asymmetric trailing edge has been successfully calculated. When employing the mass-averaged Navier-Stokes equation with two-

equation turbulence models, we found that the solutions correctly modeled all the major features of the flowfield. The solutions differed little from each other, independent of the choice of the low Reynolds number near-wall terms, the inclusion of various streamwise curvature corrections, or the choice of the two-equation model itself. When the algebraic turbulence model with special near-wake treatment was used, the solutions were not as good as those employing the two-equation models. None of the solutions correctly predicted the extent of the separated zone.

Large differences were obtained between the Navier-Stokes solutions and the boundary-layer predictions. The predicted displacement thickness distribution employing the Navier-Stokes equations was in good agreement with experimental data while the boundary-layer methods were up to 60% in error. These differences were not due to turbulence modeling, but are a result of the strong viscous/inviscid interaction process and ellipticity present in trailing-edge flows. These effects are included in Navier-Stokes flowfield solutions through the governing equations. For interactive techniques which employ boundary-layer methods, attention must be devoted to the matching process between the viscous and inviscid flowfield before adequate solutions will be obtained.

## References

[1] Melnik, R. W., Chow, R., and Mead, H. R., "Theory of Viscous Transonic Flow Over Airfoils at High Reynolds Number," AIAA Paper 77-680, Albuquerque, N. Mex., June 1977.

[2] Green, J. E., "Some Aspects of Viscous-Inviscid Interactions at Transonic Speeds and Their Dependence on Reynolds Number," AGARD-CP-83, 1971.

[3] Collyer, M. R. and Lock, R. C., "Prediction of Viscous Effects in Steady Transonic Flow Past an Airfoil," *Aeronautical Quarterly*, Vol. 30, Aug. 1979, pp. 485-505.

[4] Hurley, F. X., Spaid, F. W., Roos, F. W., Stivers, L. S. Jr., and Bandettini, A., "Detailed Transonic Flow Field Measurements About a Supercritical Airfoil Section," NASA TM X-3244, 1975.

[5] The 1980-81 AFOSR-HTTM-Stanford Conference on Complex Turbulent Flows: Comparison of Computation and Experiment, Stanford, Calif., Sept. 1981.

[6] Spaid, F. W. and Hakkinen, R. J., "On the Boundary Layer Displacement Effect Near the Trailing-Edge of an Aft-Loaded Airfoil," *Journal of Applied Mathematics and Physics*, Vol. 28, Fasc. 5, 1977, pp. 941-950.

[7] Viswanath, P. R., Cleary, J. W., Seegmiller, H. L., and Horstman, C. C., "Trailing-Edge Flows at High Reynolds Number," *AIAA Journal*, Vol. 18, Sept. 1980, pp. 1059-1065.

[8] Viswanath, P. R. and Brown, J. L., "Separated Trailing-Edge Flow at a Transonic Mach Number," *AIAA Journal*, Vol. 21, June 1983, pp. 801-807.

[9] Cebeci, T. and Meier, H. U., "Modelling Requirements for Calculation of the Turbulent Flow around Airfoils, Wings and Bodies of Revolution," AGARD-CP-271, 1980.

[10] Jones, W. P. and Launder, B. E., "The Prediction of Laminarization With a Two-Equation Model of Turbulence," *International Journal of Heat and Mass Transfer*, Vol. 15, Feb. 1972, pp. 301-314.

[11] Wilcox, D. C. and Rubesin, M. W., "Progress in Turbulence Modeling for Complex Flow Fields, Including Effects of Compressibility," NASA TP-1517, April 1980.

[12] Chien, K.-Y., "Predictions of Channel Boundary-Layer Flows with a Low-Reynolds-Number Turbulence Model," *AIAA Journal*, Vol. 20, Jan. 1982, pp. 33-38.

[13] Launder, B. E., Priddin, C. H., and Sharma, B. I., "The Calculation of Turbulent Boundary-Layers on Spinning and Curved Surfaces," *Transactions of the ASME, Journal of Fluids Engineering*, Vol. 99, March 1977, pp. 231-239.

[14] Viegas, J. R. and Horstman, C. C., "Comparison of Multiequation Turbulence Models for Several Shock Boundary-Layer Interaction Flows," *AIAA Journal*, Vol. 17, Aug. 1979, pp. 811-820.

[15] MacCormack, R. W., "A Numerical Method for Solving the Equations of Compressible Viscous Flow," *AIAA Journal*, Vol. 20, Sept. 1982, pp. 1275-1281.

[16] Ramaprian, B. R., Patel, V. C., and Sastry, M. S., "Turbulent Wake Development Behind Streamline Bodies," IIHR Rept. 231, Iowa Institute of Hydraulic Research, University of Iowa, Iowa City, July 1981.

[17] Whitfield, D. L., Swafford, T. W., and Jacocks, J. L., "Calculation of Turbulent Boundary Layers with Separation and Viscous-Inviscid Interaction," *AIAA Journal*, Vol. 19, Oct. 1981, pp. 1315-1322.